

# Nonlinear adaptive control of the NeuroMuscular Blockade in anesthesia

Margarida Martins da Silva, *Student Member, IEEE*,  
Teresa Mendonça, *Member, IEEE*, and Torbjörn Wigren, *Senior Member, IEEE*

**Abstract**—This paper presents a nonlinear adaptive control strategy based on the Wiener model for control of the NeuroMuscular Blockade in anesthesia. The structure combines the inversion of the static nonlinearity present in the Wiener model with a pole-placement controller for the linearized system. The overall strategy exploits identification of a minimally parameterized model for the description of the effect of the muscle relaxant *atracurium* in the NeuroMuscular Blockade. An Extended Kalman Filter was developed for that purpose, providing estimates of the model parameters for both the linear controller and the blocks where the inversion of the static linearity is performed. Simulations were run in a database of 100 patients simulated with the standard physiologically-based pharmacokinetic/pharmacodynamic model for the NeuroMuscular Blockade. The results show that the nonlinear adaptive controller performs well regarding reference following and tackles changes in the patient's dynamics. Noisy scenarios were also simulated to test the robustness of the proposed strategy.

## I. INTRODUCTION

Regardless of the field of application, the development of any control strategy comprises several main tasks, namely, system modeling, design of a control law, implementation and validation. Having a good mathematical model of the system becomes more and more important as the complexity of the system to be controlled increases. In biomedical applications, due to the strong parameter variability from patient to patient this requirement is particularly demanding. Moreover, since the patient dynamics may change during the time-course of the control action, an adaptive control strategy is a natural choice when dealing with control of a particular human response to external or internal excitation.

This paper presents a nonlinear adaptive control strategy, based on the Wiener model, for control of the NeuroMuscular Blockade (NMB) in anesthesia. The Wiener model consists of linear dynamics in cascade with a static nonlinear function [1]. In the anesthesia field this structure is frequently present when modeling the effect of drug administration in the human body e.g. for the NMB or the Bispectral Index (BIS). According to this structure an initial dynamic mixing of the administered drug is present in the different theoretical compartments of the human body [2], being followed by a

static transduction from the concentration of the drug in the effect site to the observed clinical effect [3]. Even though nonlinear, some advantages result from the fact that the nonlinearity is static. In particular, in controllers for Wiener type models a common strategy is to apply the inverse of the nonlinearity to the reference signal and to the measured output signal, and to design linear controllers for the obtained signals afterwards [4]. The main contribution of this paper presents a combination of this structure with adaptivity. The overall strategy also exploits the recursive identification of a new minimally parameterized model for the effect of the muscle relaxant *atracurium* in the NMB [5], [6]. This is of central importance since the excitation properties of the input (*atracurium* dose profile) are known to be poor and the number of output datapoints (NMB measurements) is small. Good results are expected to be achieved with this strategy since the main drawback of identifying and controlling an overparameterized model is not present.

Section II describes the NMB minimally parameterized model used for the system modeling and the identification strategy, an Extended Kalman Filter (EKF). Section III presents the main features of the adaptive control strategy while section IV shows the results of running the proposed strategy in a database of 100 simulated patients. Section V draws the conclusions.

## II. THE MODEL AND THE IDENTIFICATION ALGORITHM

### A. The minimally parameterized model for the NMB

A Single Input Single Output (SISO) nonlinear Wiener model (Fig. 1) describing the effect of the muscle relaxant *atracurium* in the NMB is presented here. It should be emphasized that the choice of this model with a minimal number of parameters to model the relationship between the drug and the measured effect is crucial for the success of the present adaptive control strategy [5], [6]. Moreover the units of the input and output in this minimally parameterized model comply with the standard clinical units [7].

The linear dynamic part of the model was first constructed in continuous-time and then sampled with a zero-order hold strategy [8] which enables the derivation of an EKF algorithm to estimate the underlying continuous-time parameters to be used by the adaptive controller.

In the frequency domain, the linear part of the model may be summarized by the transfer function

$$Y_l^m(s, \alpha) = \frac{k_1 k_2 k_3 \alpha^3}{(s + k_1 \alpha)(s + k_2 \alpha)(s + k_3 \alpha)} U(s), \quad (1)$$

M. M. Silva and T. Mendonça are with the Departamento de Matemática, Faculdade de Ciências da Universidade do Porto, Rua do Campo Alegre, 4169-007 Porto, Portugal, and with the UI&D Matemática e Aplicações, Departamento de Matemática, Campus Universitário de Santiago, 3810-193 Aveiro, Portugal (e-mail: {margarida.silva,tmendo}@fc.up.pt)

T. Wigren and M. M. Silva are with the Division of Systems and Control, Department of Information Technology, Uppsala University, Box 337, SE-751 05 Uppsala, Sweden (e-mail: {torbjorn.wigren,margarida.silva}@it.uu.se)

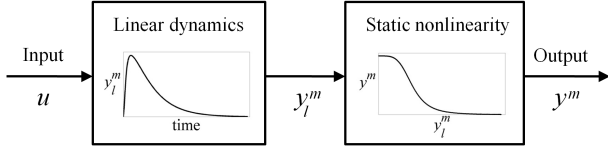


Fig. 1. The nonlinear Wiener model. The signal  $y_l^m$  is not available for measurement.

where  $Y_l^m(s, \alpha)$  is the Laplace transform of the continuous-time output  $y_l^m(t, \alpha)$  of the linear dynamic part of the model and  $U(s)$  is the Laplace transform of the input signal  $u(t)$  in Fig. 1. Here the parameter  $\alpha$  to be identified describes the inter-patients' dynamics variability. Aiming for the best modeling, the parameters  $k_i, \{i = 1, 2, 3\}$  must be chosen, noting that  $k_1 = 1$  needs to hold to get a unique parameterization. A brute force search on the available real database was performed in [9]. The combination  $k_2 = 4$  and  $k_3 = 10$  was the one that minimized the normalized error between the real and the simulated NMB signals for all cases in the real database. The constants  $k_2$  and  $k_3$  are fixed to 4 and 10, respectively, in all simulations that give rise to the results of this paper.

The static nonlinearity is modeled by the Hill equation [7]

$$r : (\gamma, y_l^m(t, \alpha)) \in ]0, +\infty[ \times ]0, +\infty[ \\ \mapsto y^m(t) = r(\gamma, y_l^m(t, \alpha)) \in ]0, 100],$$

where

$$r(\gamma, y_l^m(t, \alpha)) = \frac{100 C_{50}^\gamma}{C_{50}^\gamma + (y_l^m(t, \alpha))^\gamma}. \quad (2)$$

Here  $\gamma$  is the parameter to be identified;  $r(\cdot, \cdot)$  is a known static nonlinear function;  $y^m(t)$  is the output of the nonlinearity;  $y_l^m(t, \alpha)$  is the continuous-time output of the linear dynamic part of the model (1); and  $C_{50}$  is a normalizing constant that is kept constant during simulations, similarly to [5].

Due to the Wiener model cascade structure, and as stressed in [1], only the product of the small signal static gains of the two cascaded blocks is important from an input-output point of view. Noting that the linear part (1) contributes with a unity gain for the whole system, the differential static gain must be estimated by the parameter  $\gamma$  to be adapted in the nonlinear part (2). At the same time,  $\gamma$  adapts the shape or nonlinear static differential gain of (2). The parameter vector to be identified in the EKF structure is then selected as  $\theta = [\alpha \quad \gamma]^T$ . Hence only two parameters are estimated.

### B. Identification: the EKF algorithm

In order to implement the model structure (1), (2) in the EKF algorithm, the continuous-time representation (1) was sampled using a zero-order hold method [8].

The discrete-time model becomes

$$\begin{cases} x(kh + h) &= \Phi(\alpha) x(kh) + \Gamma(\alpha) u(kh) \\ y_l^m(kh, \alpha) &= C(\alpha) x(kh) \end{cases}, \quad (3)$$

where

$$\begin{aligned} \Phi(\alpha) &= e^{A(\alpha)h} \\ \Gamma(\alpha) &= \int_0^h e^{A(\alpha)s} ds B(\alpha). \end{aligned} \quad (4)$$

Here,  $u(kh) \in \mathbb{R}$  is the input (piecewise constant atracurium dose),  $x(kh) \in \mathbb{R}^{3 \times 1}$  is the discrete-time state-vector,  $y_l^m(kh, \alpha) \in \mathbb{R}$  is the discrete-time output of the linear block,  $\Phi(\alpha) \in \mathbb{R}^{3 \times 3}$  and  $\Gamma(\alpha) \in \mathbb{R}^{3 \times 1}$  are the sampled system matrices, and  $A(\alpha) \in \mathbb{R}^{3 \times 3}$  and  $B(\alpha) \in \mathbb{R}^{3 \times 1}$  are the continuous-time system matrices. Note that the  $k'_i s, \{i = 1, 2, 3\}$  are not shown explicitly in (3) since they are fixed in the simulations, prior to (2). Due to the fact that in the surgery environment, data from NMB is monitored and acquired every 20 seconds to ensure that all the nerve fibers are recruited every time a electrical stimulation is performed, the zero-order hold method is applied using  $h = 1/3 \text{ min}^{-1}$ .

The sampling does not affect the nonlinear block, hence (2) can be used as it is. The model output is then given by:

$$y^m(kh) = r(\gamma, y_l^m(kh, \alpha)) = \frac{100 C_{50}^\gamma}{C_{50}^\gamma + (y_l^m(kh, \alpha))^\gamma}. \quad (5)$$

To describe the EKF, the underlying general discrete-time nonlinear model is assumed to be

$$\begin{aligned} \hat{x}(t+1) &= f(t, \hat{x}(t), u(t)) + g(t, \hat{x}(t)) v(t) \\ \hat{y}(t) &= h(t, \hat{x}(t)) + e(t), \end{aligned} \quad (6)$$

where  $v(t)$  and  $e(t)$  are mutually independent Gaussian white noise sequences with zero means and covariances  $R_1(t)$  and  $R_2(t)$ , respectively. The EKF algorithm can then be summarized as follows (cf. e.g. [10]):

$$\begin{aligned} H(t) &= \left. \frac{\partial h(t, x)}{\partial x} \right|_{x=\hat{x}(t|t-1)} \\ K(t) &= P(t|t-1) H^T(t) \\ &\quad \times [H(t) P(t|t-1) H^T(t) + R_2(t)]^{-1} \\ \hat{x}(t|t) &= \hat{x}(t|t-1) + K(t) [y(t) - h(t, \hat{x}(t|t-1))] \\ P(t|t) &= P(t|t-1) - K(t) H(t) P(t|t-1) \\ \hat{x}(t+1|t) &= f(t, \hat{x}(t|t), u(t)) \\ F(t) &= \left. \frac{\partial f(t, x)}{\partial x} \right|_{x=\hat{x}(t|t)} \\ G(t) &= g(t, x) \Big|_{x=\hat{x}(t|t)} \\ P(t+1|t) &= F(t) P(t|t) F^T(t) + G(t) R_1(t) G^T(t) \end{aligned} \quad (7)$$

To enable the estimation of the model parameters with the EKF, a coupled identification model is defined. The model merges the sampled model (3) and a random walk model for the parameter estimates [11]. The resulting augmented state vector (denoted by  $\bar{x}$ ) becomes

$$\bar{x}(kh) = [x_1(kh) \quad x_2(kh) \quad x_3(kh) \quad \alpha(kh) \quad \gamma(kh)]^T. \quad (8)$$

Using (8), the extended state-space model is the following:

$$\begin{aligned} \hat{\bar{x}}(kh+h) &= \begin{bmatrix} \Phi(\hat{\alpha}(kh)) & \mathbf{0}_{3 \times 2} \\ \mathbf{0}_{2 \times 3} & I \end{bmatrix} \begin{bmatrix} \hat{x}(kh) \\ \hat{\alpha}(kh) \\ \hat{\gamma}(kh) \end{bmatrix} + \\ &+ \begin{bmatrix} \Gamma(\hat{\alpha}(kh)) \\ \mathbf{0}_{2 \times 1} \end{bmatrix} u(kh) + \begin{bmatrix} v_x(kh) \\ v_\alpha(kh) \\ v_\gamma(kh) \end{bmatrix} \end{aligned}$$

$$\begin{aligned} &\equiv \begin{bmatrix} f_1(kh, \hat{x}(kh), u(kh)) \\ \vdots \\ f_5(kh, \hat{x}(kh), u(kh)) \end{bmatrix} + v(kh) \\ &\equiv f(kh, \hat{x}(kh), u(kh)) + v(kh), \end{aligned} \quad (9)$$

$$\begin{aligned} \hat{y}^m(kh) &= \frac{100 C_{50}^{\hat{\gamma}(kh)}}{C_{50}^{\hat{\gamma}(kh)} + (\overline{C}(\hat{\alpha}(kh))\hat{x}(kh))^{\hat{\gamma}(kh)}} + e(kh) \\ &\equiv h(kh, \hat{x}(kh)) + e(kh), \end{aligned} \quad (10)$$

$$\overline{C}(\cdot) = [C(\cdot) \ 0 \ 0]. \quad (11)$$

In the EKF algorithm structure (7) it is necessary to linearize both  $f(t, x)$  and  $h(t, x)$ . The linearization of  $f(kh, \hat{x}(kh), u(kh))$  in (9) was performed analytically. The formula for  $F(kh)$  is not shown here due to its complexity. The linearization of  $h(kh, \hat{x}(kh))$  in (10) was performed numerically in order to reduce the computational complexity of the calculations:

$$H(kh) = \frac{h(kh, \hat{x}(kh) + \Delta\hat{x}(kh)) - h(kh, \hat{x}(kh))}{\Delta\hat{x}(kh)},$$

where  $\Delta\hat{x}(kh)$  is the step for the differentiation and is chosen to be small.

### III. THE ADAPTIVE CONTROLLER

#### A. Structure

The structure of the adaptive controller proposed in this paper is shown in Fig. 2 and comprises three main tasks that are performed by order at each time step: online identification of the model parameters by the EKF, inversion of the nonlinearity using the current estimate of the nonlinear parameter and linear adaptive control. The use of the online identified model parameters to linearize the Wiener model and to calculate the linear control law determines the adaptivity nature of this controller.

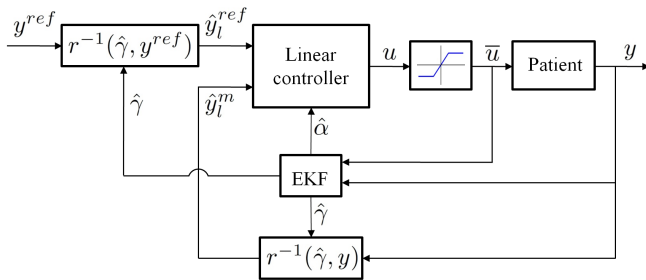


Fig. 2. Adaptive controller for the NMB minimally parameterized Wiener model.

#### B. Inversion

Both the measured NMB from the patient (output  $y$ ) and the reference value  $y^{ref}$  are first inverted through  $r^{-1}(\cdot, \cdot)$  [4] using the current estimate of  $\gamma$  provided by the EKF identification block. It should be stressed that  $r(\cdot, \cdot)$  is a bijective function and both  $y$  and  $y^{ref}$  in Fig. 2 lay inside

$[0, 100]$  as consequence of monitoring restrictions of the NMB in the clinical practice. Moreover, as a result of a projection algorithm in the EKF structure [5],  $\hat{\gamma}$  is also lower-bounded. Due to this, and considering the domains affecting  $r(\cdot, \cdot)$  (2), no problems arise in this inversion. Ideally, when  $\gamma$  is accurately estimated and no disturbances are present,  $r(\hat{\gamma}, \cdot)$  is a perfect model of the static nonlinearity and the loop becomes linear. The static nonlinearity of the system is then canceled exactly by  $r^{-1}(\hat{\gamma}, \cdot)$  which means that the output of the linear block of the Wiener system appears directly as input for the linear controller. The linear part of the controller is therefore designed to control the output of the linear dynamic part of the Wiener type system as if there was no static nonlinearity. For the linear control a continuous-time pole placement strategy with integral action is used [4]. This allows the linearized control error to be regulated away. This then also regulates away differences between the reference  $y^{ref}$  and the output  $y$  since the same inverting function is applied to both these signals.

#### C. Linear Control Design

According to (1), and following the notation in [4], pp. 93, the patient continuous-time linear dynamics is given by

$$A(s) \hat{y}_l^m(t) = B(s) u(t) + w(t), \quad (12)$$

where  $A(s) = (s + k_1 \alpha)(s + k_2 \alpha)(s + k_3 \alpha)$ ,  $B(s) = k_1 k_2 k_3 \alpha^3$ , and  $w(t)$  is a disturbance. The idea is to require that the response from the command signal  $\hat{y}_l^{ref}(t)$  (here being the linear reference signal to be followed) to the output  $\hat{y}_l^m(t)$  be described by the dynamics

$$A_m(s) \hat{y}_l^m(t) = B_m(s) \hat{y}_l^{ref}(t). \quad (13)$$

with  $A_m(s) = (s + p_{m1})(s + p_{m2})(s + p_{m3})$  and  $B_m(s) = b_{m0}$  since  $\deg A_m(s) = \deg A(s)$  and  $\deg B_m(s) = \deg B(s)$ .

The admissible control laws enabling the achievement of such requirements are given by [4], pp. 93,

$$R(s) u(t) = T(s) \hat{y}_l^{ref}(t) - S(s) \hat{y}_l^m(t). \quad (14)$$

In order to design such a causal control law, a factorization of  $B(s)$  must be performed as  $B(s) = B^+(s) B^-(s)$ , where  $B^+(s)$  is a monic polynomial whose zeros are stable and  $B^-(s)$  corresponds to unstable or poorly damped factor that cannot be canceled. Due to the fact that there are no process zeros to be canceled in (12),  $B^+(s) = 1$  and  $B^-(s) = B(s)$ . Since  $\deg B(s) = \deg B_m(s) = 0$ ,  $B_m(s) = \beta B(s)$  where  $\beta = A_m(0)/B(0)$ . The closed-loop characteristic polynomial is  $A_c(s) = A_o(s) A_m(s)$  with  $A_o(s) = (s + p_{o1})(s + p_{o2})$ , and the Diophantine equation to be solved with respect to the unknowns  $R(s)$  and  $S(s)$  becomes [4], pp. 94,

$$A(s) R(s) + B(s) S(s) = A_c(s) = A_o(s) A_m(s). \quad (15)$$

As in [12], and since the adaptive controller applies the same inverting transformation to the measured output  $y$  and to the reference value  $y^{ref}$ , the controlled output

will approach any constant reference setpoint provided that the controller has integral action, and that the closed loop remains stable. To enforce stability in practice, the closed-loop poles are kept in the stable region by a parameter projection into the set of stable models, *cf.* e.g. [1]. The condition of having integral action in the controller aims to regulate away any static error that may be present in the controlled signal  $\hat{y}_l^m(t)$ . This static error regulation is captured by assuming that the disturbance  $w(t)$  in (12) is generated by  $A_d(s)w(t) = e(t)$ , where  $e(t)$  is continuous-time white noise and  $A_d(s) = s$ . In terms of pole placement controller design this means that an additional stable closed-loop pole  $X(s) = s + x_0$  has to be added to the adaptive controller structure [4], pp. 124. The new polynomial  $R^0(s)$  will be given by  $R^0(s) = A_d(s)R^0(s)$ . Hence, if  $R(s)$  and  $S(s)$  are solutions to (15),

$$R^0(s) = X(s)R(s) + Y(s)B(s) \quad (16)$$

$$S^0(s) = X(s)S(s) - Y(s)A(s) \quad (17)$$

will satisfy [4], pp. 123,

$$A(s)R^0(s) + B(s)S^0(s) = X(s)A_c(s). \quad (18)$$

From (16) it follows that

$$R^0(s) = sR^0(s) = (s + x_0)R(s) + y_0B(s), \quad (19)$$

with  $x_0$  to be chosen and  $Y(s) = y_0$  obtained by making  $s = 0$  in (19):

$$y_0 = -\frac{x_0 R(0)}{B(0)}. \quad (20)$$

Inserting  $X(s)$  and  $y_0$  into (16) and (17) the new controller is found. The complete control law is then given by

$$R^0(s)u(t) = T(s)\hat{y}_l^{ref}(t) - S^0(s)\hat{y}_l^m(t), \quad (21)$$

resulting in a closed-loop system of order 6.

#### D. Anti-windup

Due to the nature of the problem to be solved,  $u(t)$  must be nonnegative and below a predefined maximum  $u_{max}$ . Moreover, knowing that controllers with integral action may perform poorly in the presence of actuators that saturate [4], pp. 128, the control law (21) was further augmented with an anti-windup strategy (depicted in Fig. 2). Rewriting (21) in the observer form and describing the saturation in the input as

$$\bar{u}(t) = \begin{cases} 0, & \text{if } u(t) < 0 \\ u(t), & \text{if } 0 \leq u(t) \leq u_{max} \\ u_{max}, & \text{if } u(t) > u_{max} \end{cases} \quad (22)$$

the control law avoiding windup is then given by [4], pp. 456,

$$A_0(s)u(t) = T(s)\hat{y}_l^{ref}(t) - S^0(s)\hat{y}_l^m(t) + (A_0(s) - R^0(s))\bar{u}(t). \quad (23)$$

The control law (23) was discretized using the zero-order hold method in [8] to obtain the drug dose to be given to the simulated patient in each time instant.

## IV. SIMULATION RESULTS

A number of simulations were carried out to test the performance of the proposed nonlinear adaptive controller. Each simulated patient was chosen from a bank of 100 models that was randomly generated in [13] assuming a lognormal probability distribution for the 8 parameters present in the standard physiologically-based Pharmacokinetic/Pharmacodynamic (PK/PD) model. Following clinical procedures, a *bolus* of *atracurium* ( $500 \mu\text{g kg}^{-1}$ ) was assumed to be given to each simulated patient at  $t = 0$  min, making the NMB to drop from its initial value of 100% to a value around 0% in less than 10 minutes after administration.

The design of the adaptive strategy is such that the controller is only turned on at the beginning of the recovery from the initial *bolus* ( $t \approx 30$  min [14]). This patient-dependent time instant is calculated online by the OnLine tuned Algorithm for Recovery Detection [15] that is coupled to the adaptive controller structure (not shown in Fig. 2).

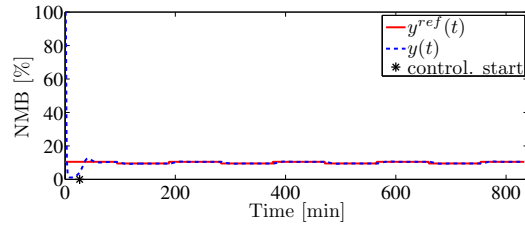
For simulation purposes, the EKF is initialized as in [6] with

$$\hat{x}(0|-1) = [0 \ 0 \ 0 \ 0.03 \ 1]^T. \quad (24)$$

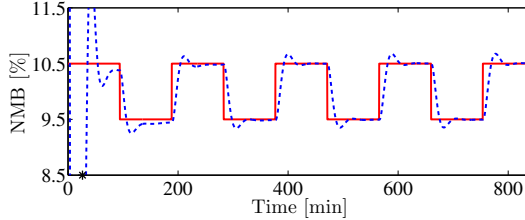
The value of  $R_2$  is chosen as different from [6] and varies depending on the scenario for simulation, among the three that were tested.

*Example 1:* The first scenario assesses the nonlinear adaptive controller performance in a noiseless situation. Here  $R_2 = 10^3$ . The reference profile  $y^{ref}(t)$  to be followed is a square wave of amplitude 0.5% around the setpoint of 10% with period equal to  $60\pi$ . Some simulation results for case number 98 in the database for this first scenario are presented in Fig. 3. The roots of polynomials  $A_m(s)$ ,  $A_o(s)$  and  $X(s)$  are chosen such that the output signal of all cases in the database behave similarly and are  $-0.7$ ,  $-0.6$ ,  $-0.3$ ,  $-0.8$ ,  $-0.4$ , and  $-0.8$ , respectively. In Fig. 3(a) and 3(b) it is clear that the output signal  $y(t)$  follows the reference  $y^{ref}(t)$ . The static error present at the beginning of the simulation is regulated away with time, as expected due to the presence of integral action in the controller. This reference tracking is possible due to the control signal shown in Fig. 3(c). The peaks of dose exist whenever the reference changes, being in the admissible range of drug administration for *atracurium*. The parameter estimates for this case, calculated by the EKF are shown in Fig. 3(d) and 3(e).

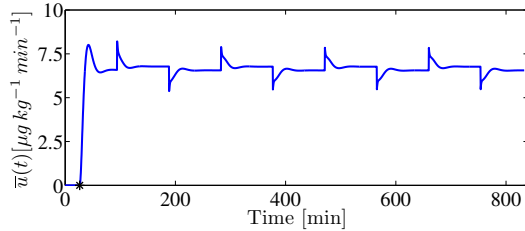
*Example 2:* The adaptive capability of the designed adaptive controller is evaluated in the second simulation scenario. The parameters of the standard physiologically-based PK/PD model of case number 98 in the model bank are used to simulate the patient until  $t = 333$  min. After that, the parameters of the simulated patient model are changed of 20%. It is expected that the controller tackles this change in the model parameters, still following the reference signal  $y^{ref}(t)$  (constant in a level of 10%). The pole locations of the controller are the same as in Example 1. As it is clear in Fig. 4(a) the output signal  $y(t)$  tracks the reference  $y^{ref}(t)$  after the controller is turned on. The adaptation of the controller to the new patient parameters is shown in Fig. 4(b) through



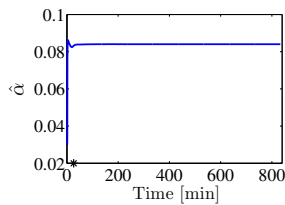
(a) Reference signal  $y^{ref}(t)$  and output signal  $y(t)$ .



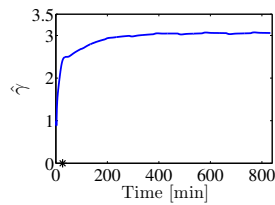
(b) Zoom of (a).



(c) Control signal (atracurium dose).



(d) Estimates of  $\alpha$ .

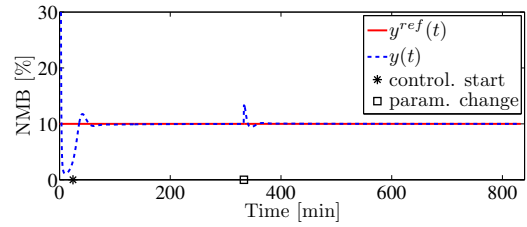


(e) Estimates of  $\gamma$ .

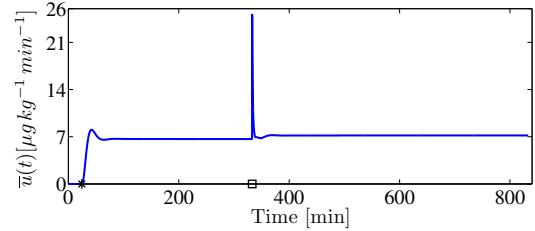
Fig. 3. Results for case number 98 in the database using the nonlinear adaptive controller with  $p_{m1} = 0.7$ ,  $p_{m2} = 0.6$ ,  $p_{m3} = 0.3$ ,  $p_{o1} = 0.8$ ,  $p_{o2} = 0.4$ , and  $x_0 = 0.8$ . The star mark in the  $x$ -axis indicates the time instant when the controller started.

one instantaneous change in the control action around minute 333. This is consequence of the significant change in the parameters estimates provided by the EKF as adaptation to the new conditions (Fig. 4(c) and 4(d)).

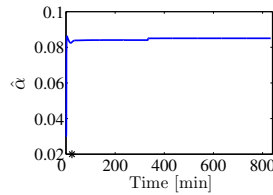
*Example 3:* The third scenario aims to assess the performance of the nonlinear adaptive controller in the presence of noise. At this stage, a NMB record from a typical real patient was chosen from a database of cases previously collected in the surgery room [5], [9]. The EKF algorithm described in [6] was applied to this case and the residuals obtained after this identification step are used as the noise vector to be added to the output signal in simulation. Due to the presence of noise, the value of  $R_2$  associated with the error in the output signal is chosen as  $2 \times 10^3$ . In the simulations whose results are shown in Fig. 4 the roots of polynomials  $A_m(s)$ ,  $A_o(s)$  and  $X(s)$  are  $-0.7$ ,  $-0.6$ ,  $-0.05$ ,  $-0.8$ ,  $-0.4$ , and  $-0.1$ ,



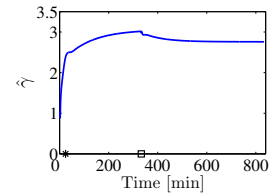
(a) Reference signal  $y^{ref}(t)$  and output signal  $y(t)$ .



(b) Control signal (atracurium dose).



(c) Estimates of  $\alpha$ .



(d) Estimates of  $\gamma$ .

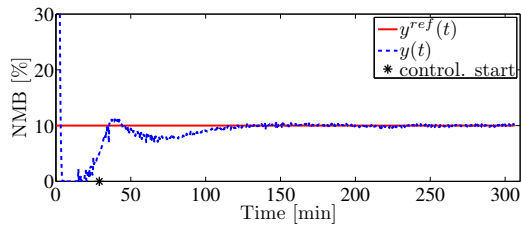
Fig. 4. Results for case number 98 in the database using the nonlinear adaptive controller with  $p_{m1} = 0.7$ ,  $p_{m2} = 0.6$ ,  $p_{m3} = 0.3$ ,  $p_{o1} = 0.8$ ,  $p_{o2} = 0.4$ , and  $x_0 = 0.8$ . The star mark in the  $x$ -axis indicates the time instant when the controller started and the square mark indicates the time where the patient parameters were changed.

respectively;  $x_0$  takes the value of 0.1 in order to smooth the control action. In Fig. 5(a) it is clear that the output signal  $y(t)$  follows the reference signal  $y^{ref}(t)$ , constant in 10%. The oscillation in the output signal after the controller is turned on (with maximum value of 12% and minimum of 7%) is clinically accepted. The control signal  $\bar{u}(t)$  in this example is displayed in Fig. 5(b) and the parameter estimates obtained by the EKF in Fig. 5(c) and 5(d).

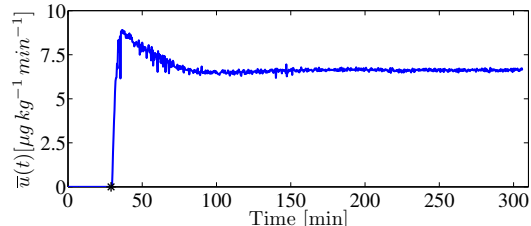
These results show the ability of the developed nonlinear adaptive controller in steering the NMB (output signal) to a desired reference, tracking a certain constant or varying profile. The proposed controller structure, taking advantage of the identification of the minimally parameterized model for the NMB [6], is also able to deal with parameter-varying systems, as Fig. 4 indicates. Equally important is the good performance of the nonlinear adaptive controller in the presence of measurement noise, which is crucial when testing this structure in real environments.

## V. CONCLUSIONS AND FUTURE WORK

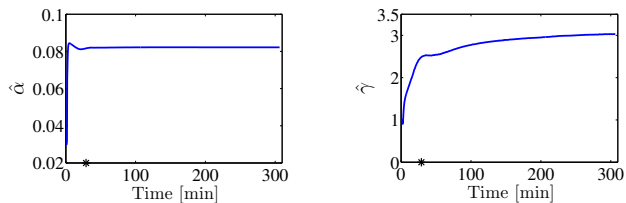
Even though many different strategies for the control of the NeuroMuscular Blockade have been developed, analyzed and implemented both in simulation and in real clinical situations during the past years e.g. [13], [16], [17], the features of the problem mainly the high inter- and intra-patient variability



(a) Reference signal  $y^{ref}(t)$  and output signal  $y(t)$ .



(b) Control signal (atracurium dose).



(c) Estimates of  $\alpha$ .

(d) Estimates of  $\gamma$ .

Fig. 5. Results for case number 98 in the database using the nonlinear adaptive controller with  $p_{m1} = 0.7$ ,  $p_{m2} = 0.6$ ,  $p_{m3} = 0.05$ ,  $p_{o1} = 0.8$ ,  $p_{o2} = 0.4$ , and  $x_0 = 0.1$ , and with the addition of noise. The star mark in the  $x$ -axis indicates the time instant when the controller started.

and the restrictions imposed by the clinical practice suggest the development of different approaches.

The novelty of the strategy proposed in this paper is the use of a minimally parameterized model for the description of the effect of the muscle relaxant *atracurium* in the NeuroMuscular Blockade [6] and the incorporation of an online identification strategy (an Extended Kalman Filter) in the controller structure, providing adaptivity to the nonlinear controller. As a consequence the variability of the patient parameters does not interfere with the performance of the controller. Moreover, this new strategy constitutes one reliable alternative to the use of a finite number of patient models to switch from [17]. Since stability conditions are monitored by the Extended Kalman Filter, the controller is hence able to cover a continuous-range of patient nonlinear behaviors. It should also be stressed that the proposed adaptive controller addresses the control of the NeuroMuscular Blockade in a highly realistic scenario, exemplified by the third scenario of simulation where noise present in a real record collected in the surgery room is added to the output signal. The good results obtained in simulation are strong indications that the proposed nonlinear adaptive controller will behave well when implemented in a real control situation.

In order to guarantee total patient safety and before implementing this adaptive control strategy in real control

platform, further work has to be developed to screen convergence and stability properties of the proposed closed-loop structure. This nonlinear adaptive controller is also highly promising when extended to other nonlinear Wiener responses in anesthesia, namely the Bispectral Index.

## VI. ACKNOWLEDGMENTS

The authors gratefully acknowledge the support of Fundação para a Ciência e a Tecnologia through the individual grant with reference SFRH/BD/60973/2009 and the project Galeno with reference PTDC/SAU-BEB/103667/2008. The research leading to these results has also received funding from the European Research Council under the European Community's Seventh Framework Programme (FP7/2007-2013)/ERC grant agreement n°247035.

## REFERENCES

- [1] T. Wigren, "Recursive prediction error identification method using the nonlinear Wiener model," *Automatica*, vol. 29, no. 4, pp. 1011–1025, 1993.
- [2] K. Godfrey, *Compartmental models and their application*. Academic Press, 1983.
- [3] H. Derendorf and B. Meibohm, "Modeling of pharmacokinetic/pharmacodynamic (PK/PD) relationships: Concepts and perspectives," *Pharmaceutical Research*, vol. 16, pp. 176–185, 1999.
- [4] K. J. Åström and B. Wittenmark, *Adaptive Control, 2nd ed.* Mineola, New York, USA: Dover Publications, Inc., 2008.
- [5] M. M. Silva, T. Wigren, and T. Mendonça, "Nonlinear identification of a minimal neuromuscular blockade model in anaesthesia," Dept. Information Technology, Uppsala University, Uppsala, Sweden, Tech. Rep. 2009-023, Available: <http://www.it.uu.se/research/publications/reports/>, Sept. 2009.
- [6] —, "Nonlinear identification of a minimal neuromuscular blockade model in anaesthesia," *IEEE Trans. Contr. Sys. Tech. (in press)*, Jan. 2011.
- [7] B. Weatherley, S. Williams, and E. Neill, "Pharmacokinetics, pharmacodynamics and dose-response relationships of atracurium administered i. v.," *Br. J. Anaesth.*, vol. 55, pp. 39s–45s, 1983.
- [8] K. J. Åström and B. Wittenmark, *Computer-Controlled Systems*. Englewood Cliffs, NJ: Prentice Hall, 1984.
- [9] M. M. Silva, "Prediction error identification of minimally parameterized nonlinear Wiener models in anaesthesia," in *Proc. of the 18th IFAC World Congress*, Milan, Italy, Aug 28-Sep 2 2010, pp. 5615–5620.
- [10] T. Söderström, *Discrete-time Stochastic Systems*. London, UK: Springer-Verlag, 2002.
- [11] T. Söderström and P. Stoica, *System Identification*. Hemel Hempstead, UK: Prentice-Hall, 1989.
- [12] T. Wigren and L. Brus, "Reduction of amplitude dependent gain variations in control of non-linear Wiener type systems," in *Proc. of the 7th IFAC Symposium on Nonlinear Control Systems*, Pretoria, South Africa, 2007, pp. 730–735.
- [13] P. Lago, T. Mendonça, and L. Gonçalves, "On-line autocalibration of a PID controller of neuromuscular blockade," in *Proc. of the 1998 IEEE Inter. Conf. on Control Applications*, Trieste, Italy, 1998, pp. 363–367.
- [14] H. Mellinshoff, L. Radbruch, C. Diefenbach, and W. Buzello, "A comparison of cisatracurium and atracurium: onset of neuromuscular block after bolus injection and recovery after subsequent infusion," *Anesthesia & Analgesia*, vol. 83, no. 5, pp. 1072–1075, 1996.
- [15] M. M. Silva, C. Sousa, R. Sebastião, J. Gama, T. Mendonça, P. Rocha, and S. Esteves, "Total mass TCI driven by parametric estimation," in *Proc. of the 17th Mediterranean Conference on Control and Automation (MED'09)*, jun. 2009, pp. 1149–1154.
- [16] P. Oliveira, J. P. Hespanha, J. M. Lemos, and T. Mendonça, "Supervised multi-model adaptive control of neuromuscular blockade with off-set compensation," in *Proc. of the 2009 European Contr. Conf. (ECC'09)*, Aug. 2009, pp. 3064–3069.
- [17] T. Mendonça, J. M. Lemos, H. Magalhães, P. Rocha, and S. Esteves, "Drug delivery for neuromuscular blockade with supervised multimodel adaptive control," *IEEE Transactions on Control Systems Technology*, vol. 17, no. 6, pp. 1237–1244, nov. 2009.